PARTICLE TRI-AXIAL ROTOR MODEL CALCULATION FOR NEGATIVE PARITY LOW-LYING STATES OF ODD-A ISOTOPES OF MERCURY

BY

SHALLO FEKADU

A THESIS SUBMITTED TO JIMMA UNIVERSITY COLLEGE OF NATURAL SCIENCES DEPARTMENT OF PHYSICS IN PARTIAL FULFILLMENT OF THE REQUIREMENTS FOR THE DEGREE OF MASTERS OF SCIENCE IN PHYSICS (NUCLEAR PHYSICS)

June 2019

DECLARATION

I hereby declare that this M.Sc thesis entitled"Particle Tri-Axial Rotor Model Calculation for Negative Parity Low-Lying States of odd-A Isotopes of Mercury" is my original work and has not been presented for a degree in any other university, and that all sources of material used have been duly acknowled.

Name: Shallo Fekadu

Signature: ——————

This M.Sc thesis has been submitted for examination with my approval as university advisor.

Name: Dr. Teklemariam Tessema

Signature: ——————

Place and Date of Submission:

Jimma University

Department of Physics

June 2019

Acknowledgement

First of all, I would like to thank the almighty God, for every blessing things he did for me. Then I will express my heartfelt gratitude and respect to my advisor and instructor, Dr. Teklemariam Tessema, for his unwavering and inspirational support and guidance, not only in this carrier, but also throughout my life. In general, for what he plant's in my heart, even for the rest of my race.

Again, I would like to extend my respected thank to my gift of God, beloved wife, Kidist Asnake, for all of your patience, and sacrifice you paied in caring my flourish kids and families as well. Yes, you have been a source of hope, strength and inspiration. Hence, you were always injecting me some sort of energy, to overcome every challenge during this period.

I am also thankful to Jimma University and the Department of Physics at Jimma University for sponsoring my study.

Finally, I would like to extend my limitless appreciation and thank to all of my instructors (now colleagues) and all staffs, for your support in all of my study carrier in one or another way.

Shallo Fekadu

June 2019.

Abstract

Low-Lying states in the odd-mass Hg isotopes, $^{(197,199,201)}Hg$, have been investigated in the framework of the Particle Plus Tri-Axial Rotor Model (PTRM). To perform these calculations, the computer codes GAMPN, ASYRMO, and PROBAMO were used. Thereby, all 15 negative-parity single-neutron orbitals in the deformed, $N = 82$–126, shell were taken into account and the standard set of Nilsson parameters κ and μ was employed. Theoretical calculations of the nuclear structure parameters, like Level Energies, Gamma Transition Energy, Transition Intensity (Branching ratio), Electromagnetic transitions(EM_1 and EM_2) and Magnetic transitions BM_1 were made. The intrinsic and collective states are determined by using the deformed mean field of Nilsson and the monopole-pairing interaction (BCS). The level schemes of odd-mass Hg isotopes, $^{(197,199,201)}Hg$, are discussed and compared with the already existing experimental data. In all aspects of the considered calculations, the result were in a reasonably good agreement with the already existing experimental data with an error less than 8% in average.

Contents

List of Figures

List of Tables

1

Introduction

1.1 Background of the Study

Nuclear physics is a young science dating back to the discovery of radioactivity in 1896 $[1, 33]$. Since then a lot of works have been done in the area in different time by different scholars. Particularly, after the beginning of modern nuclear physics, 1932, many problems in atomic structure including the low-lying states of odd-mass isotopes of different nuclei were solved experimentally by the application of quantum mechanics and nuclear physics $[1]$.

Moreover, during the last twenty-five years the progress in nuclear physics has been very rapid. The development of new experimental techniques, especially the development of high-energy accelerators and different nuclear structure models has resulted in very extensive studies of nuclear phenomena involving stable as well as artificially radioactive nuclei. The intensive study of nuclear structure was also one of the achievement of this period. Actually because of the typical property of the nucleus it was not as such easy task $[2]$.

The structure of atomic nuclei depends on the interactions of its constituents; protons, and neutrons. These interactions play a key role in the development of configuration mixing and in the onset of collectivity and deformation, in changes to the single

particle energies and magic numbers, and in the microscopic origins of phase transitional behavior.

Till date, the study of nuclear structure is very interesting and crucial in the field of Nuclear Science, which generates from the properties of the nucleus. That is, atomic nucleus is a strongly-interacting, many-body quantum mechanical system that exhibits a fascinating variety of shapes and excitation modes, from spherical to super deformed (axis ratio $2:1$), and from excitations of single protons and neutrons to collective vibrations and rotations of the nucleus as a whole [5], this by itself is very interesting and attractive property to investigate, what is going on inside the nucleus and to study about the nuclear structure as well, especially in the mass region of, $150 < A < 220$, which is a crucial testing ground for the nuclear models aspiring at the description of such complex nuclear structure [1].

In addition, the study of nuclear structure attempts to elucidate the unifying mechanisms by which these rich patterns of behavior emerge from the common underlying strong nuclear interaction between the nucleons (protons and neutrons) that form the nucleus. Central to these studies, the concept of nuclear shell structure, in which protons and neutrons occupy quantized energy levels within a potential generated by their interactions with all of the other nucleons is very intersting [5].

Moreover, the study of nuclear structure in the negative parity low-lying states of different isotopes is one of the recent direction of nuclear scientists, by developing different models. Hence, they had worked to investigate about the nuclear structure experimentally by measuring, its descriptive parameters; Level Energies, Gamma Transition Energy, Transition Intensity (Branching Ratio), Electromagnetic transitions(EM_1 and EM_2) and Magnetic transitions BM_1 etc.

Mercury is one of the interesting nucleus in that, its isotopes are situated in a transi-

tional region, which lies above the region of deformed prolate, rare earth nuclei and just below the spherical lead nuclei $Z = 82$ [4]. The low- lying structure of odd-A Mercury isotopes with two proton holes with respect to $Z = 82$ shell closure are expected to be dominated by the available single particle neutron orbitals near $N = 126$ shell closure. The heavier Mercury isotopes has a small oblate deformation and show various interesting properties [3].

In this thesis, the negative parity low-lying states of odd-mass Hg isotopes have been addressed, by reducing its many body quantum mechanical system in to two body system, in the framework of the Particle plus Tri-Axial Rotor Model (PTRM), by performing theoretical calculations of the nuclear structure parameters.

1.2 Statement of the Problem

So far, there were experimental data's published regarding negative parity low-lying states of odd-mass Hg isotopes [22, 34]. To the best of my knowledge, there were no theoretical data published based on the Particle Tri-Axial Rotor Model calculation for the low-lying negative parity states of Mercury isotopes, $^{(197,199,201)}Hg$.

But, for the maximum benefit from the nucleus, we need to have explicit information about it, both theoretically as well as experimentally.

Based on this gap, in this thesis an attempt was made to calculate the low-lying negative parity states of odd-mass Mercury isotopes, that guided by the following research questions.

- What are the calculated values of Gamma transition energies, Electric and Magnetic transition probabilities?
- What is the schematic descriptionof the level energies?

- What is the result of the Gamma intensity branching ratio of each transition?
- How is the agreement between theoretically calculated and experimentally measured data?

1.3 Objectives

1.3.1 General Objective

The ultimate goal of this effort is to theoretically study the negative parity low-lying states of odd-A Mercury isotopes based on the Particle Tri-Axial Rotor Model, and compare the results with the already existing experimental value(data).

1.3.2 Specific Objectives

Any investigative task has its own particular objectives to be achived. Hence, this thesis also set the following as its ultimate specific goals.

- To calculate values of Gamma transition energies and Electric and Magnetic transition probabilities.
- To obtain Gamma intensity branching ratio of each transition.
- To give explicit explanation about the level scheme and all the calculated values by comparing with the already existing experimental data.

1.4 Significance of the Study

As this study aimed to investigate about nuclear structure at low states of Mercury isotopes in the transition region, it has meaningful importance to the area and to the related field as well. Some of these are;

- It will give theoretical data and description on negative parity low-lying states of odd-A Mercury isotopes.
- It can be used as a reference by other researchers.
- It will initiate young researchers towards the area.

1.5 Limitation of the Study

Inorder to make this work fruitful as this, there were a lots of ups and downs to be faced, even some of them were hindered the work not to sucessed more than this. These are;

- Shortage of published references on the theoretical work.
- Lack of advanced Nuclear physics laboratory, to carry out an experiment by myself rather than taking literature data to compare with.
- Insufficient budget to go to advanced nuclear laboratories abroad and to participate in different experiance sharing workshopes.

2

Review of Related Literature

2.1 Nuclear Structure

2.1.1 Introduction

The atomic nucleus is a strongly-interacting, many-body quantum mechanical system that exhibits a fascinating variety of shapes and excitation modes. Like the atom, it has discrete energy levels. The locations of the exited states differ for each nucleus are characterized by quantum numbers that describes its angular momentum, parity and isospin [5].

The past thirty years have brought great strides in our understanding of the structure of nuclei. Such techniques as Coulomb excitation, nucleon-transfer reactions, in-beam spectroscopy, elastic and inelastic scattering, and radioactive decay have been used to probe the nature of nuclear structure. Along with these experimental efforts, theoretical nuclear models have been developed in an effort to explain and predict the experimental results and understand the properties of nuclei. The goal of this effort is to account for the complex properties of nuclei in terms of nucleon-nucleon interactions. However, a fundamental microscopic description of the nucleus is lacking, numerous approximate nuclear models have been proposed in attempts to explain the three broad classes of nuclei.

1. Spherical, closed shell nuclei

2. Highly deformed nuclei, many nucleons removed from closed shells, and

3. Transitional nuclei, lying between these two extremes.

The first model which was successfully predicted nuclear properties for a broad range of nuclides was the shell model developed in the late $1940'$s by Mayer, Haxel, Jensen, and Suess [6]. This model assumed that the motion of each nucleon was completely independent of that of the other nucleons and could be described by using a harmonic oscillator potential which included strong spin-orbit coupling. The latter when added to earlier versions of this model permitted realization of a quantitative reproduction of nuclear properties, replacing the limited qualitative picture that had previously existed. The shell model is quite successful in its prediction of various nuclear properties; such as spins, parities, magnetic moments for odd-mass nuclei, magic numbers, and alpha and beta decay energy systematics.

Despite these accomplishments, its scope is severely limited. Nuclei far from closed shells had properties that were not fully explained; specifically, the existence of large static quadrupole moments and energy levels far below the individual particle excitations, and the enhancement of electric quadrupole transition rates. The first successful explanation of these aspects came in the early $1950'$s with the realization by Bohr and Mottelson, that these properties are characteristic of collective nucleonic motion in nuclei with permanently deformed ground states. Classically, these collective motions correspond to shape oscillations of the nuclear surface or rotations of the nucleus as a rigid or a fluid body. Shape oscillations (the so-called "vibrational" model) have had much success in describing nuclei near the closed shells, where as a rotational descrip-

tion (the ”rotational” model) has proved applicable to highly deformed nuclei far from closed shells. Neither model does very well, however, for the regions between these two extremes, i.e. the so-called transitional region where nuclei are only slightly deformed, and asymmetric shapes have been shown, to play an important role [18].

Microscopic extensions and refinements of the classical vibrational model have been applied to the study of nuclei in transitional regions. The most widely used formalisms involve the use of particle vibration coupling. However, numerical calculations with these models, despite their complexity, have met with only limited success in interpreting transitional nuclei. The rotational model has also been extended in attempts to reproduce the properties found in transitional regions. The rotation-alignment model and tri axial rotor model have produced surprisingly good results for interpreting unmixed unique parity high-spin orbitals in regions where the original rotational model was long thought to be invalid. A complete description of nuclear properties for nuclei in transitional regions has not yet been found in terms of rotational degrees of freedom. The most physically realistic model for transitional nuclei may involve a combination of rotational and vibrational modes, but such a model has not yet been devised [24].

2.1.2 Nuclear Shell Model

Shell model was an attempt to reproduce the observed magic numbers and to explain the unusual stability of nuclei having these number of similar nucleons. The basic assumption of this model is that each nucleon is moving inside the nucleus in an average potential due to the other nucleons. Central to these studies is the concept of nuclear shell structure, in which protons and neutrons occupy ordered and quantized energy levels (stable quantum states) within a potential generated by their interactions with

all of the other nucleons [16]. The energy levels are filled in accordance with the Paulis exclusion principle. Each energy level has an upper limit $2(2l+1)$ for the number of nucleons that can be accommodated. This model gives large energy gaps between particular groups of levels forming closed shells which exhibits extra stability. The proton number and neutron number corresponding to the shell closures are known as magic numbers. All the paired nucleons form an inert core and the nuclear properties are attributed to the unpaired valence nucleons [5].

Many nuclei behave as if most of the nucleons from an inert core and low-lying exited states are determined by a few nucleons outside the core. The picture is similar to that of an atom in which electrons are arranged in shells and any chemical activity is determined by the most weakly bound, valance electrons [4]. By the independent particle model, we refer to the description of a nucleus in terms of non-interacting in the orbits of a spherically symmetric potential $V(r)$, which itself is produced by all the nucleons, and the quantized energy levels cluster into groups or shells, and the filling of major energy shells leads to particularly stable configurations associated with the proton and neutron "magic numbers": $2, 8, 20, 28, 50, 82,$ and 126, which also experimentally determined by a sharp drop in neutron and proton separation energy. Nuclei near closed shells tend to have spherical ground states, while those far from shell closures are deformed and exhibit low-energy collective rotational excitations.

In considering an appropriate potential for the nuclear case, a tremendous simplification results obtained, if the potential is central, i.e. if it depends only on the radial distance from the origin to the given point. We denote an arbitrary potential by $V(r)$ and only require that $V(r)$is attractive and $V(r) = 0$ as $r \to \infty$. Then the

Hamiltonian of a nucleus is:

$$H = \sum_i (T_i + V(r_i)) + \lambda[\sum_{i,j,i\neq j} V(r_{ij}) - \sum_i V(r_i)]. \tag{2.1}$$

The Central potential($V(r_i)$)>> Residual potential ($\lambda[\sum_{i,j,i=j} V(r_{ij}) - \sum_i V(r_i)]$) $\Rightarrow \lambda \to 0$

The Schrodinger equation for the motion of a particle in a mean spherically symmetric potential [23] is:

$$\hat{H}\psi = E\psi. \tag{2.2}$$

Single particle Hamiltonian operator:

$$\hat{H} = \frac{-\hbar^2}{2M}\nabla^2 + V(r). \tag{2.3}$$

Then, introducing Eq. (2.3) in to Eq. (2.2) and rearanging we can get:

$$\frac{-\hbar^2}{2M}\psi(r) + [E - V(r)]\psi(r) = 0, \tag{2.4}$$

where,

- E - is the energy Eigen value of any nucleon (neutron or proton)
- m - is its mass $= m_n$ or m_p
- $\psi(r)$ - is the wave function of a nucleon, and
- $V(r)$ - is the potential energy of a nucleon

The general solution of Eq. (2.4) is:

$$\psi_{nlm}(r, \theta, \varphi) = \psi_{nl}(r) Y_{lm}(\theta, \varphi), \tag{2.5}$$

with, n, l and m being the quantum numbers to determine eigen states corresponding to E_{nl}. Since the exact nature of nuclear potential is unknown, various types of potentials are taken as approximations.

2.1.3 Nuclear Deformation

For nuclear physicists, nuclear shapes and deformations have been interesting topics, since the identification of nucleus. The highly complicated nature of structure and properties of nuclei may be one of the reasons for this. Moreover, shape is one of the fundamental properties of nuclei. Till date, no theory is developed to describe the nuclear structure and properties completely, because, the knowledge about the forces, which shape the nucleus is very limited [16]. The configuration dependent forces present inside the nucleus is mainly the nuclear force between nucleons and Coulomb force between protons. The shell effects and pairing correlation also contribute to the determination of nucleonic configuration. The atomic nuclei exhibit spherical, quadruple and higher order multipole deformed shapes, even though the quadruple deformed shapes are mostly discussed. Due to the interplay between single particle and collective degrees of freedom, the coexistence of different shapes at the same spin and similar energies is also not rare [23].

Nuclei having spherical shape in their ground state are few in number. The deformed nuclei are classified into prolate, oblate and tri-axial. Prolate and oblate nuclei are axially symmetric. If the third axis of the nucleus is longer than the others, the nucleus is prolate and if it is shorter, the nucleus is oblate. For tri-axial nuclei, the three axes are different. In nature, prolate nuclei dominate over oblate ones. It is found that 86% of the even-even nuclei are prolate in the ground state and tri-axial shapes are very rare for them [30]. The effect of Coulomb repulsion between protons is to deform the nucleus more into an elongated shape than to a flattened shape. The difference in the volume element of the collective coordinates between prolate and oblate shapes is pointed out to be another reason for the prolate dominance over oblate shape. The

spin-orbit potential (coupling) between nucleons plays a role favoring stable prolate shape for nuclei [17]. The shell structure of nuclei is also responsible for the variety of shapes, depending on the position of Fermi level between two closed shells. Prolate shape occurs just after closed shells and towards the end of closed shells, oblate shape is observed.

The nuclear deformation is characterized by two collective parameters, the deformation parameter β or ϵ and the tri-axiality . Positive and negative quadruple deformations β_2 or ϵ_2 correspond to prolate and oblate shapes respectively. For$\gamma = 60^0, 0, -60^0 and -120^0$, the nucleus is axially symmetric and it is tri-axial for all other values. $\gamma =, 0$ and 60^0 represent prolate and oblate shapes respectively. The variation of nuclear shapes with respect to deformation and tri-axiality parameters are illustrated in Fig.(2.1). Depending on the extent of deviation from spherical symmetry, the deformed nuclei fall into different groups. Nuclei with major to minor axis ratio around $(1.3 : 1)$ are normally deformed and those with $(1.5 : 1)$ are highly deformed. If the ratios are $(2 : 1)$ and $(3 : 1)$, the nuclei are super deformed (SD) and hyper deformed respectively. Nuclear deformation which is the departure from spherical shape without density change is expressed in terms of the shape parameters $\alpha\lambda\mu$ and spherical harmonics $Y^{\mu}_{\lambda}(\theta, \Phi)$ [17, 18, 19] as Eq. (2.6).

$$R(\theta, \phi) = R_0[1 + \sum_{\lambda\mu} \alpha_{\lambda\mu}(t) Y^{\mu}_{\lambda}(\theta, \phi)], \tag{2.6}$$

Where, $R(\theta, \phi)$ is the distance of the nuclear surface at angles θ and ϕ from the center and R_0 is the radius at spherical equilibrium.

For each mode of order λ, μ has $(2\lambda + 1)$ values. I.e., from $-\lambda$ to $+\lambda$,

- $\lambda = 1$, corresponds to dipole oscillation,
- $\lambda = 2$, to quadrupole oscillation, and

- $\lambda = 3$, to octupole oscillation [11].

For quadrupole shapes,

$$R = R_0[1 + \sum_{2\mu} \alpha_{2\mu}(t) Y_2^{\mu}(\theta, \phi)]. \tag{2.7}$$

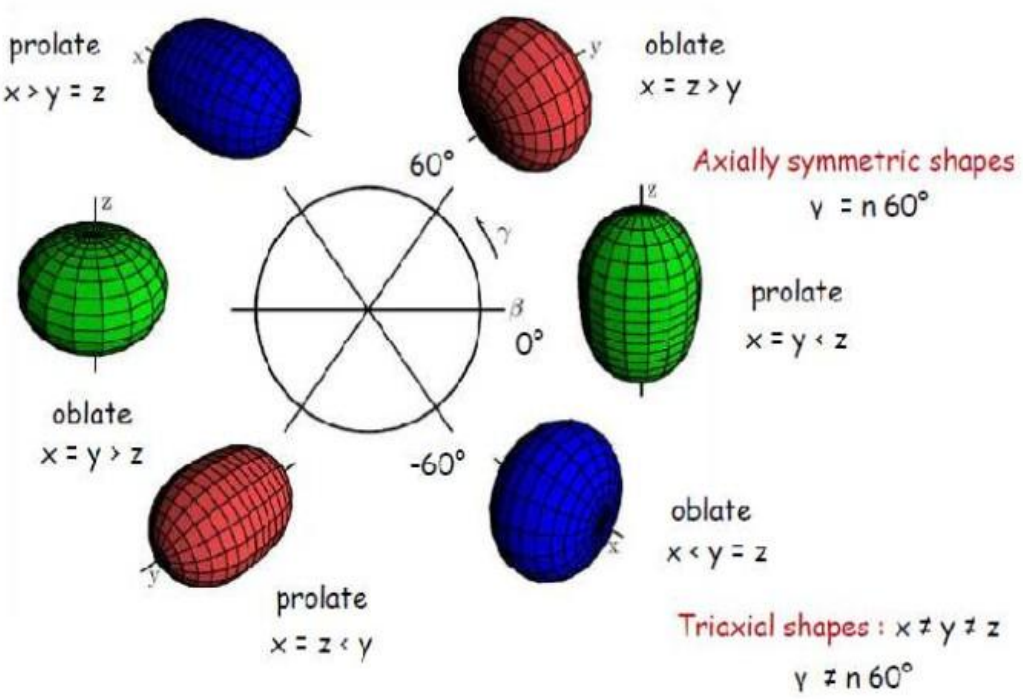

Figure 2.1: Variation of nuclear shapes with deformation and tri-axiality parameters

.

The quadrupole deformation parameter β_2 and the triaxiality γ are defined [18, 24] as:

$$\alpha_{20} = \beta_2 cos\gamma. \tag{2.8}$$

$$\alpha_{22} = \alpha_2{}_{-2} = \frac{1}{\sqrt{2}} \beta_2 sin\gamma. \tag{2.9}$$

So that,

$$\sum |\alpha_{22}|^2 = (\beta_2)^2. \tag{2.10}$$

$$\alpha_{20} = \beta_2 cos\gamma. \tag{2.11}$$

$$\alpha_{22} = \alpha_2{-}_2 = \frac{1}{\sqrt{2}}\beta_2 sin\gamma. \tag{2.12}$$

Since, $\alpha_{21} = \alpha_{2-1} = 0$. ϵ_2 is defined [31] as:

$$\epsilon_2 = \frac{R_{major} - R_{minor}}{R_0}. \tag{2.13}$$

And the quadrupole deformations β_2 and ϵ_2 are related by:

$$\epsilon_2 = 0.95\beta_2. \tag{2.14}$$

The deformation leads to change in potential energy surface (PES) of the nucleus. Thus the calculation of PES can give information about the nature of shape evolution taking place in nuclei at high angular momentum. At the minimum potential energy (PE), the nucleus will be in equilibrium. Hence the deformation corresponding to the minimum PE decides the shape of the nucleus in its ground state [18].

In the case of a spherical nucleus, according to the shell model, the energy states are grouped into different shells and there is a large separation between these shells. Nuclei with closed shells are having magic number of protons and neutrons and are stable in their ground state. Then by solving the Schrdinger equation for a spherical potential well, all the energy states are known. When there are partially filled shells, the nucleus is deformed and energy states are different from those for a spherical well. But as the deformation is increased to super deformation, it is found that new energy levels are

grouped together showing shell closure property with a different set of magic numbers.

Stable deformed nuclei are common in the rare earth (lanthanides: $50 < Z < 82, 82 < N < 126$) and transuranic elements (actinides:$Z > 82, N > 126$). Light nuclei having partially filled shells are also deformed. Super deformed nuclei were first found in the region of nuclear mass $A = 150, 190$ and $A > 220$. In the periodic table, nuclei with mass number $A > 220$ are super deformed in their ground state. Many super deformed nuclei are discovered in distinct regions with mass number around $60, 90, 130, 150, 190$ and 240. In the mass range $50 < A < 190$ and $A > 220$, the nuclei are found to be deformed in their ground state [26].

2.1.4 Square well potential

Square well potential [19] is of the form:

$$V(r) = -U_0, r \leq R. \tag{2.15}$$

$$V(r) = \infty, r > R. \tag{2.16}$$

Using this infinite square well potential, the radial part of the solution of Schrodinger equation are spherical [23] Bessel functions:

$$U_{nl}(r) = j_l(kr) = r^{\frac{-1}{2}} J_{l+\frac{1}{2}}(kr), \tag{2.17}$$

With,

$$k = \sqrt{\frac{2ME}{\hbar^2}}. \tag{2.18}$$

The Eigen values are obtained as:

$$E_{nl} = \frac{\hbar^2 k_{nl}^2}{2M}. \tag{2.19}$$

The particle occupancy for a level l is $2(2l + 1)$ and the closed shells occur with proton and neutron numbers $\sum 2(2l + 1)$. According to the shell model with square well

potential, the predicted proton and neutron numbers corresponding to shell closure are $2, 8, 18, 20, 34, 40, 58, 68, 70, 92, 106, 112, 138$ and 156. But the experimentally observed magic numbers are $2, 8, 20, 50, 82$ and 126. i.e., this model could reproduce only the three observed magic numbers $2, 8$ and 20 [23].

2.1.5 Harmonic oscillator potential well

This potential in particular is popular in nuclear physics, because,

- It provides a remarkably good approximate solution to many nuclear problems and
- It is particularly easy to handle mathematically, thus yielding many results analytically, and is given [16] by:

$$V(r) = \frac{1}{2}m\omega^2 r^2. \tag{2.20}$$

where ω is the classical frequency of the oscillator. With the potential in Eq. (2.20), the Schrodinger equation in Eq. (2.4) leads to the differential equation, for the radial part [23].

$$\frac{-\hbar^2}{2\mu}\frac{d^2\psi}{dr^2} + [V(r) + \frac{\hbar^2 l(2l+1)}{2\mu r^2}]\psi_{nl}(r) = E\psi_{nl}(r), \tag{2.21}$$

With,

$$\psi_{nl}(r) = rU_{nl}(r). \tag{2.22}$$

Its solutions have some interesting properties. First, outside the potential, the wave function decreases exponentially and therefore vanishes as $r \to \infty$. The quantum number n specifies the number of nodes(zeros) of the wavefunction with the usual, but not

universal convention that one counts the node at infinity but not that at$r = 0$, that is, $n = 1, 2, ...$

The solution of Eq. (2.21) becomes:

$$\psi_{nl}(r) = N_{nl}e(^{\frac{-1}{2}vr^2})r^{l+1}U_{nl}(r), \tag{2.23}$$

Where, $v = \frac{M\omega}{h}$ and $U_{nl}(r)$, is the Laguerre polynomial. Then the normalized eigen functions are:

$$\psi_{nl}(r) = \frac{\psi_{nl}(r)}{r}Y_{nl}(r). \tag{2.24}$$

and the corresponding eigen values are:

$$E_{nl} = \hbar\omega(2n + l - \frac{1}{2})orE_n = \hbar\omega(N + \frac{3}{2}), \tag{2.25}$$

Where, $N = N_x + N_y + N_z = 1, 2, 3...$, the orbital quantum number $l = 0, 1, 2, 3, ...$ and $N = 2n + l - 2$.

The degeneracy corresponding to each l value is $2(2l + 1)$. The eigen states corresponding to the same value of $2l + 1$ are also degenerate $[16]$.

Then the accumulating total number of particles for all levels up to N is:

$$\sum_N N_N = \frac{1}{3}(N + 1)(N + 2)(N + 3). \tag{2.26}$$

In the shell model using Harmonic oscillator potential well, the nucleon numbers corresponding to the shell closures are calculated as: $2, 8, 20, 40, 70, 112$ and 168. Here also the experimentally observed magic numbers above 20 are not reproduced.

The energy levels of the harmonic oscillator potential given in Fig. (2.3) below shows, the energy level degeneracys, and a given state generally contains more than one value of the principal quantum number and of the orbital angular momentum l. It is this grouping of levels that provides the shell structure required of any central potential useful for real nuclei. If we recall that each energy level has $2(2l + 1)$degenerate m

states, then, by the Pauli Principle, each level can contain $2(2l+1)$particles. Therefore, if we imagine filling such a potential well with fermions, each group or shell can contain, at most, the specific number of particles indicated in the Fig. (2.3).

Hence, such a potential automatically gives a shell structure rather than, a uniform distribution of levels. Unfortunately, except for the lowest few, these shells do not correspond to the empirical magic numbers $[9, 19]$. The harmonic oscillator potential is a reasonable first order approximation to the appropriate nuclear potential, but it needs further improvement.

2.1.6 Spin-orbit potential

In the 1940s, many unsuccessful attempts were made at finding the needed correction; success was finally achieved by Mayer, Haxel, Suess, and Jensen who showed in 1949 that the introduced an additional spin-orbit term to the centrally symmetric potential, which gives the proper separation of the sub shells and produce the empirical magic numbers. The spin-orbit potential is proportional to $l.s$ and its introduction causes the splitting of the $j \pm \frac{1}{2}$ levels $[8, 16]$.

This gives significant change in the energy level by splitting it and showing fine structure, particularly at higher energy level, the higher orbital angular momentum levels are brought down in energy. So far neither of these produce the magic numbers experimentally. According to Mayer and Jensen the strong spin-orbit potential included to explain magic numbers is given by;

$$V(r) = V_{central}(r) + V_{so}(r)l.s, \tag{2.27}$$

Where, V_{so} is negative and $V_{so} = V_{ls}(r)l.s$.

The $l.s$ factor causes the reordering of the levels. With a spin-orbit component, the force felt by a given particle is differs according to whether its spin and orbital angular

momenta are aligned parallel or antiparallel. If it is parallel the V_{so}term affects higher l values more. As in atomic physics, in the presence of a spin-orbit interaction, it is appropriate to label the states with the total angular momentum quantum number [27].

$$j = l + s. \tag{2.28}$$

A single nucleon has, $s = \pm\frac{1}{2}$, hence the possible values of j are, $j = l + \frac{1}{2}$ or $j = l - \frac{1}{2}$ (except for $l = 0$ for which $j = \frac{1}{2}$ is allowed).

The expectation value $\langle l.s\rangle$is obtained from:

$$j^2 = (l+s)^2 = l^2 + 2l.s + s^2 \rightarrow l.s = \frac{1}{2}(j^2 - l^2 - s^2), \tag{2.29}$$

$$\langle l.s\rangle = \frac{\hbar^2}{2}[j(j+1) - l(l+1) - s(s+1)], \tag{2.30}$$

$$V_{so} = V_{ls}(r)\frac{\hbar^2}{2}l, for j = l + \frac{1}{2}. \tag{2.31}$$

$$V_{so} = -V_{ls}(r)\frac{\hbar^2}{2}(l+1), for j = l - \frac{1}{2}. \tag{2.32}$$

And the energy separation is the difference of $\langle l.s\rangle$ for each state:

$$\langle l.s\rangle_{j=l+\frac{1}{2}} - \langle l.s\rangle_{j=l-\frac{1}{2}} = \frac{\hbar^2}{2}(2l+1). \tag{2.33}$$

The energy splitting increases when l increases. For $V_{ls}(r) < 0$ the member of the pair with the larger $j, (j = l + \frac{1}{2})$ is pushed downward. This level is now in the gap between the second and third shells, where its capacity of 8 nucleons gives the magic number 28. The p and d splitting do not result in any major regrouping of levels. The next major effect of the spin-orbit term is on the $1g$ level. The $1g_{\frac{9}{2}}$ state is pushed down to the next lower major shell; its capacity of 10 nucleons adds to the previous total of 40 for that shell to give the magic number of 50. A similar effect occurs at the top of each major shell. In each case the lower energy member of the spin-orbit pair from the next shell is pushed down into the lower shell, and the remaining magic numbers follow exactly as

expected $[8, 10]$.

Results in energy splitting of individual levels for a given J (angular momentum) is:

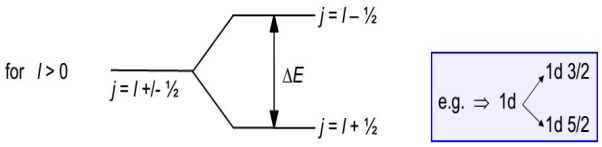

Figure 2.2: Energy splitting for an individual J .

$V_{central}$ with $(L.S)$, $\triangle E = \frac{1}{2}(2l+1)V_so$, larger j lies lower.

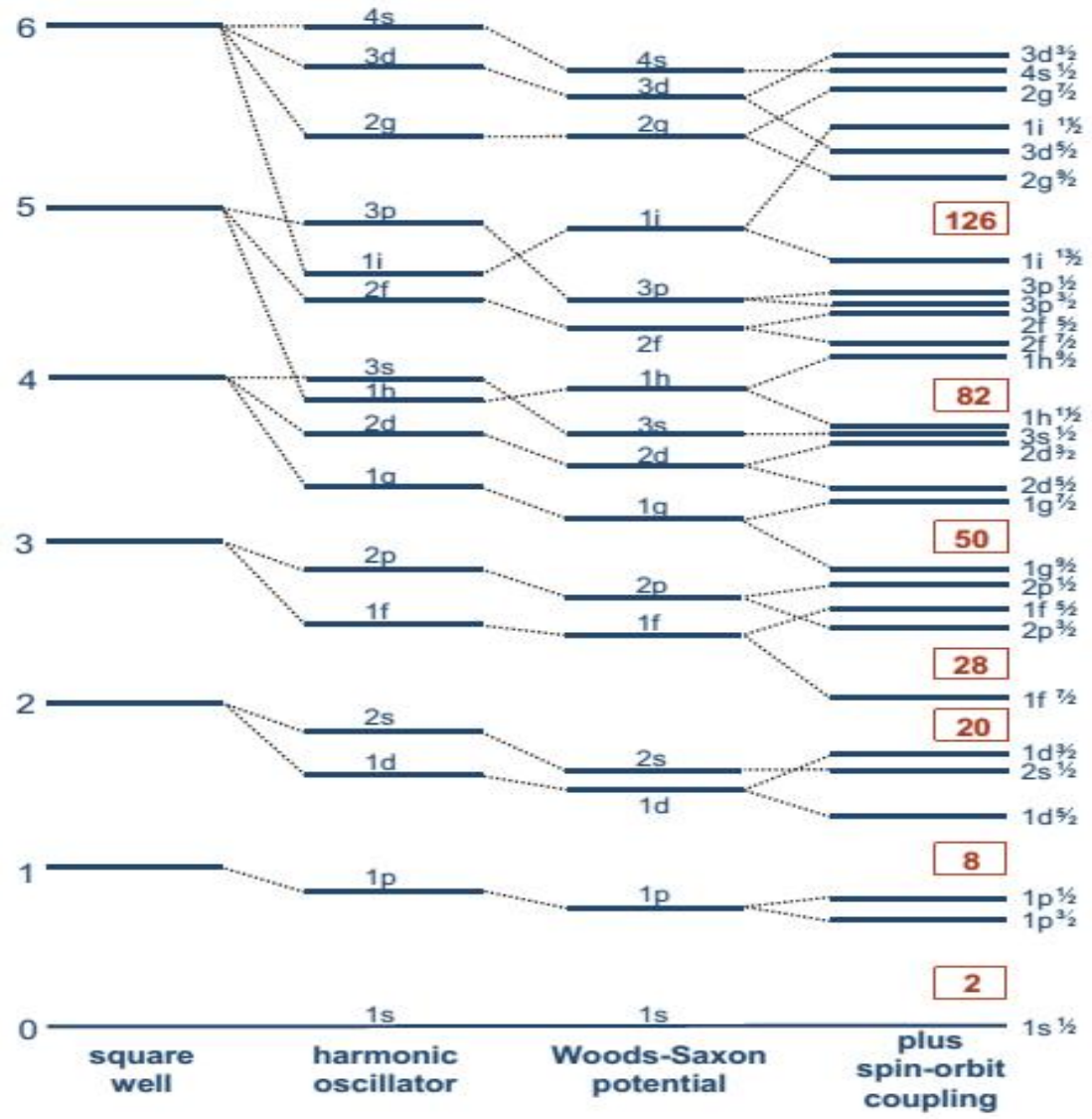

Figure 2.3: Energy level splitting for the determined potentials.

The spherical shell model with spin-orbit coupling and an l^2 term succeeded in justifying the observed shell closures and the energy Eigen values. But in nature most of the nuclei show deviation from spherical symmetry and appreciable quadrupole moments are noticed in different regions of the periodic table. The reason is the polarization of the closed core by the valence nucleons. In order to describe such nuclei, the present shell model is to be modified. Nilsson succeeded in tackling the problem of deformed nuclei by some modifications to the spherical shell model, the details of which is discussed under the section Collective models.

Due to the enormous dimension of the configuration space involved, it is not practically possible to use spherical shell model for heavy nuclei. A variational approach to the shell model represented by Monster and Vampir calculations may be adopted to get rid of from this situation. This variational shell model calculations can be performed in the case of medium mass and heavy nuclei [9].

2.1.7 Nilsson potential

To incorporate the effects of deformation in nuclear properties, Nilsson modified the shell model by introducing a self-consistent deformed potential instead of a spherically symmetric harmonic oscillator potential. The modified single particle oscillator potential Nilsson used is, the axially symmetric oscillator potential with spin-orbit coupling and a term proportional to l^2. Thus the triaxial single particle Nilsson Hamiltonian is given as [16]:

$$H = H_0 + Cl.s + Dl^2, \tag{2.34}$$

Where,

$$H_0 = -\frac{\hbar^2}{2m}\bigtriangledown'^2 + \frac{1}{2}m(\omega_x^2 x'^2 + \omega_y^2 y'^2 + \omega_z^2 z'^2), \tag{2.35}$$

With, x', y' and z' being the coordinates in a frame fixed with the nucleus. Taking cylindrical symmetry, the deformation parameter ϵ_2 is introduced in such a way that [11, 32]:

$$\omega_x = \omega_y = \omega_0(1 + \frac{1}{3}\epsilon_2), \tag{2.36}$$

And

$$\omega_z = \omega_0(1 - \frac{2}{3}\epsilon_2), \tag{2.37}$$

With, $\omega_x\omega_y\omega_z$= Constant, Which is the condition for constant volume of the nucleus. Then ω_0 and ϵ_2 related [23] as:

$$\omega_0^0(\epsilon_2) = \omega_0^0(1 - \frac{4}{3}\epsilon_2^2 - \frac{16}{27}\epsilon_2^3)^{-\frac{1}{6}}, \tag{2.38}$$

With, ω_0^0 bing the value of ω_0 for spherical nucleus. The deformation parameters ϵ_2 andβ_2 are related as:

$$\epsilon_2 = \frac{3}{2}\sqrt{\frac{5}{4\pi}}\beta_2. \tag{2.39}$$

2.1.8 Particle Tri-Axial Rotor Model

This model used a tri-axial rotor to explain the low-lying states in some transitional nuclei. The model can also be extended to odd mass nuclei by the coupling of an external particle to a tri-axial rotor at the same time, it describes various general features of rotating systems. In the particle tri-axial rotor model, the Hamiltonian of the system is given[34] by:

$$H = H_{cor} + H_{sp} + H_{pair}. \tag{2.40}$$

The single-particle Hamiltonian H_{sp} describes the odd particle in a deformed Woods-Saxon potential characterized by the deformation parameters β_2 , and β_4 . For the Woods-Saxon potential we used the parameterization. As a first step, the single-particle energies and wave functions are calculated. From the generated Nilsson states in the cylindrical basis $\Omega N n_z \Lambda$, a set is selected which is used to construct the particle plus rotor strong-coupling basis states. The single-particle matrix elements necessary for the particle plus rotor Hamiltonian and the calculation of transition strengths are computed within this set. In Eq. (2.40), H_{pair} represents the pairing force acting between like nucleons and is treated within the Bardeen- Cooper- Schrieffer (BCS) approximation. Thereby, a Fermi level λ, a pairing gap $\triangle$ and the quasi-particle energies are derived.

The core (even-even core) Hamiltonian of Eq. (2.40) has the form:

$$H_{cor} = \sum \frac{\hbar^2 {R_i}^2}{2J_k} = \sum \frac{\hbar^2 (I_k - j_k)^2}{2J_k}, \tag{2.41}$$

Where, R, I and j are the angular momentum of the core, the nucleus and the single particle, respectively [14].

The three rotational moments of inertia J_k of Eq. (2.41) are assumed to be connected by a hydro dynamical type relation as:

$$J_k = \frac{4}{3} J_0 sin^2(\gamma + \frac{2\pi}{3}k), \tag{2.42}$$

Where, $k = 1, 2, 3$, the fixed moment of inertia J_0 can be divided from the core excitation energy E_2^+, H_{sp} describes the Hamiltonian of the unpaired single particle. In the tri-axial deformed field of the even-even core, H_{sp} in Eq. (2.40), is given by:

$$H_{sp} = -\frac{\hbar^2}{2m}\bigtriangledown^2 + \frac{1}{2}m\omega_0^2 1 - 2\beta[Y_{20}cos\gamma + \frac{1}{\sqrt{2}}(Y_{20} + Y_{2-2})sin\gamma] - k\hbar\omega_0 2l.s + \mu(l^2 - \langle l_N \rangle^2), \tag{2.43}$$

Where, k and μ are Nilsson parameters, $Y_{2q}$is the rank 2 spherical harmonic function[34]. H_{pair} is the Hamiltonian to represent the pairing correlation which can be treated in the Bardeen- Cooper- Schrieffer (BCS) formalism. The single particle wave function can be expressed as [13]:

$$|v\rangle = \sum C^v_{Nlj\Omega} |Nlj\Omega\rangle, \tag{2.44}$$

Where

- v-is the sequence number of the single particle orbitals.
- $|Nlj\Omega\rangle$ - is the cross-ponding Nilsson state.
- $C^v_{Nlj\Omega}$ - is the coefficient to identify the configuration mixing.

Diagonalizing the single particle Hamiltonian in the basis $|Nlj\Omega\rangle$ we can obtain the $C^{v}_{Nlj\Omega}$ and the single particle eigen value ε_v.

The total Hamiltonian in Eq. (2.40) can be diagonalized in the symmetrically strong coupling basis.

$$|IKMv\rangle = \sqrt{\frac{2I+1}{16\pi^2}}[D^{I}_{MK}\alpha^{+}_{v}|0\rangle + (-1)^{(I-K)}D^{I}_{(M-K)}\alpha^{+}_{v}|0\rangle], \tag{2.45}$$

Where, α^{+}_{v} creation of the single nucleon in the orbital $|v\rangle$, D^{I}_{Mk}, is the rotational matrix [19].

2.1.9 Nuclear Magnetic Dipole Moment

The magnetic moment of a nucleus is induced by the orbiting charged particles (the protons) giving rise to an orbital magnetic field (characterized by g_l and by the intrinsic spin $S = \frac{1}{2}$) of the nucleons, inducing their own intrinsic magnetic field (characterized by g_s). The dipole operator, expressed in terms of these two contributions is given by:

$$\mu = \sum_{i=1}^{A} g^{i}_{l} l^{i} + \sum_{i=1}^{A} g^{i}_{s} s^{i}, \tag{2.46}$$

where, the spin g factors are known to be for the electron, proton, neutron and muon [35].

The free-nucleon gyro magnetic factors for protons and neutrons are$g^{(p)}_{1} = 1, g^{(n)}_{1} = 0, g^{(p)}_{1} = +5.587, g^{(n)}_{1} = -3.826$. The magnetic dipole moment μ_I is the expectation value of the z-component of the dipole operator μ [32]: $(I) = \langle I, m = I|\mu_z|I, m = I\rangle$ It is related to the nuclear spin I via the gyromagnetic ratio g_l: $\mu = g_l I \mu_N$, with $\mu_N$being the nuclear magneton and given by:

$$\mu_N = \frac{e\hbar}{2m_p}. \tag{2.47}$$

Which is defined in terms of the single charge of the proton, e, and its mass, m_p. Its current measured value is $\mu_N = 5.05078324(13) \times 10^{27} \frac{J}{T}$.

Within the shell model the properties of odd-A nuclei near closed shells are described by the characteristics of the unpaired valence nucleon. The magnetic moment of such a nuclear state with its valence nucleon in an orbit with total angular momentum j and orbital momentum l,can be calculated as a function of the free-nucleon g-factors, and they are called the Schmidt moments:

$$\mu(l + \frac{1}{2}) = \lfloor (j - \frac{1}{2})g_l + \frac{1}{2}g_s \rfloor \mu_N. \tag{2.48}$$

$$\mu(l - \frac{1}{2}) = \frac{j}{j+1}[(j - \frac{3}{2})g_l - \frac{1}{2}g_s]\mu_N. \tag{2.49}$$

In a real nucleus the magnetic moment of a nucleon is influenced by the presence of the other nucleons. This can be taken into account by using effective proton and neutron g-factors to calculate the effective single-particle magnetic moment $\mu(lj)^{eff}$ for a nucleon in a particular orbit [10].

2.1.10 Nuclear Electric Quadrupole Moment

The nuclear electric quadrupole moment Q_s of a nuclear state with spin I is a measure of the deviation of the nuclear charge distribution from sphericity. A non-zero quadrupole moment indicates that the charge distribution is not spherically symmetric. The classical denition of the charge quadrupole moment in a Cartesian axis system is given [36] by:

$$Q_z = \sum_{i=1}^{A} Q_z(i) = \sum_{i=1}^{A} e_i(3Z_i^2 - r_i^2), \tag{2.50}$$

with, $e_i$being the charge of the respective nucleon and (x_i, y_i, z_i) its coordinates. By convention, from Eq. (2.50), if $Q > 0$ the shape is prolate and if $Q < 0$ Oblate.

The spectroscopic quadrupole moment can be related to an intrinsic quadrupole

moment Q_0 reflecting the nuclear deformationβ , in an assumption that, the nuclear deformation is axially symmetric with the nuclear spin having a well-defined direction with respect to the symmetry axis of the deformation (strong coupling). In this case, the intrinsic and the spectroscopic quadrupole moment are related as follows:

$$Q_s = \frac{3K^2 - I(I+1)}{(I+1)(2I+3)} Q_0, \tag{2.51}$$

with, K being the projection of the nuclear spin on the deformation axis(z-axis). This intrinsic quadrupole moment Q_0, induced by the non-spherical charge distribution of the protons, can then be related to the nuclear charge deformation as follows $[12, 28]$:

$$Q_0 = \frac{3}{\sqrt{5\Pi}} ZR^2\beta(1 + 0.36\beta). \tag{2.52}$$

2.1.11 Rotational Bands in Deformed Nuclei

The most collective bands known in nuclei are the rotational bands that occur wherever the nuclear shape becomes appreciably non spherical. Such shapes are due to the shell effects in nuclei. When a shell is filled there is extra stability. So that, for the usual (spherical) shell model, a spherical shape is stabilized near closed shells. However, between shells the spherical shape is disfavored and the nucleus deforms in order to find a more favorable energy. Such deformations give rise to an orientation degree of freedom for the nucleus and thereby to the possibility of rotation. A rotational band reflects a very simple type of collective motion, which changes the orientation of the system without essentially affecting its shape or internal structure. The energy associated with the motion is mainly kinetic and written as:

$$E = \frac{1}{2} l\omega^2 = \frac{\hbar^2}{2l} I(I+1), \tag{2.53}$$

Where, the value of l, the moment of inertia, depends on the shape and internal structure, $\omega$is the angular velocity, and I is the angular momentum. This energy relationship

expresses one of the most characteristic features of nuclear rotational motion and applies to the rotation of any near-rigid symmetric top. It works even better for diatomic molecules. It is interesting that all the low-lying excitation modes of a nucleus have analogs in a diatomic molecule. Both systems have rotational, vibrational, and particle excitations, with energy scales for the particle excitation (electronic vs. nucleonic) that differ by about 10^6 (eV to MeV). In the molecular case the three modes differ from each other in energy by factors of approximately 50, so they are almost independent (the adiabatic hypothesis works well). However, the (low-lying) nuclear vibrational energies are of the same order as single particle excitations, indicating that this vibrational mode does not become strongly collective in nuclei [20].

2.1.12 Gamma Transition selection rule

As a nucleus performs electromagnetic transition from higher energy state to lower energy state it emits photon that carries out an angular momentum of J and parity π, and must be conserved. If the angular momenta of the initial and final states of final nucleus can be labeled as $J_i\hbar$ and $J_f\hbar$ and change in intrinsic angular momentum, $\triangle\ J(\hbar)$ is of course $l = \triangle\ J = (J_i - J_f)\hbar$. If $\triangle\ J = 0$, is forbidden for single photon emission, at least it has to have a minimum intrinsic spin $l\hbar$ units to connect the two nuclear states. For a multipole transition to be possible we will use the so called γ-ray selection rules which results from the laws of conservation of angular momentum and parity, and is given as:

$$|J_i - J_f| \leqslant L \leqslant |J_i + J_f|. \tag{2.54}$$

Parity, π is

For, $\pi^f = \pi^i(-1)^L$, E_L is Electric multipole transition

For, $\pi^f = \pi^i(-1)^{(L+1)}$, M_L is Magnetic multipole transition

Based on the angular momentum and parity change between the initial and the final state the γ-ray decays are classified according to their multipolarity L and the character π [10].

3

Materials and Methodology

3.1 Materials

In order to achive the ultimate goal of this thesis, the following materials were used in one or the other way intensively. I.e. survey of related Literatures, Books, Experimental Data's, Computers, Fortran based Computational Codes (GAMPN, ASYRMO and PROBAMO), the particle tri-axial rotor model.

3.2 Methodology

3.2.1 Analytical Method

Simple calculation of the modified harmonic oscillator potential, branching ratios, level energy differences, etc. which is used in the determination of nuclear structure was done in bold.

3.2.2 Computational Method

Using the Particle Tri-Axial Rotor Model Code's, which is Fortran based computational code, theoretical calculation of the nuclear structure parameters was performed with the aid of the following three consecutive computer programs. These are;

i. Program GAMPN

- Used to calculate the single particle energies, wave functions and matrix elements.
- The input includes deformation parameters and Nilsson parameters (K, μ).

ii. Program ASYRMO

- The input data will be taken from GAMPN, and
- It diagonalizes the particle plus tri axial rotor Hamiltonian in strong coupling basis, with the single particle matrix elements.

iii. Program PROBAMO

- The input data for single particle quantities will be from GAMPN and for particle rotor quantities will be from ASYRMO.
- It will calculate both diagonal and off diagonal matrix elements (static moments, transition rates, mixing ratios etc.) [22].

3.2.3 Method of Data Presentation

- The data obtained from the Particle Tri-Axial Rotor Model (PTRM) calculation has been plotted as a nuclear level structure for the negative parity low-lying odd-mass isotopes of Mercury, $^{(197,199,201)}Hg$ one by one, and data tabulation also made in parallel.
- Simultaneously, the experimental data was also plotted.
- Then, comparison between the theoretical and experimental plot have been made.
- Based on the obtained data, theoretical explanation have been made in advance.

4

Result and Discussion

In the present work, the particle plus tri-axial rotor model (PTRM) was used to study the negative parity low-lying state of odd-A mercury isotopes, by coupling a proton to the remaining even-even core of the nucleus.

First, the single-particle energies and wave functions corresponding to the modified harmonic oscillator (MHO) potential are calculated for a fixed quadrupole deformation(ϵ, γ). From the generated Nilsson states, a set is selected which is used to construct the particle plus rotor strong-coupling basis states. With in this set of orbitals all single-particle matrix elements necessary for the particle plus rotor Hamiltonian and the calculation of transition strengths are computed.

As a next step, the particle plus tri-axial rotor Hamiltonian matrix is constructed and diagonalized. Then, electromagnetic matrix elements, both diagonal and off-diagonal, are calculated with the wave functions obtained.

In addition, for the successful accomplishment of the particle plus tri-axial rotor model (PTRM) calculations, the computer codes GAMPN, ASYRMO, and PROBAMO were used [22]. Thereby, all 15 negative-parity single-neutron orbitals in the deformed, $N = 82 - 126$, shell were taken into account and the standard set of Nilsson parameters κ and μ was employed. The calculation of the negative parity low-lying state nuclear structure parameters was achieved with the selected optimal values of the mercury iso-

topes of their respective deformation parameters as shown below. In doing so, the Coriolis effect were neglected and some parameters kept at their standard values.

i. For $^{197}_{80}Hg$

A deformation parameter (ϵ_2) for the even-even core $^{196}_{80}Hg$ is; $\epsilon_2 = 0.290$ and $\gamma = 32^0$. A value of $\Delta = 0.78MeV$ was obtained by the BCS calculation for the pairing gap. For the Fermi level, that calculation yielded, $\lambda_F = 52.3644MeV$.

ii. For $^{199}_{80}Hg$

A deformation parameter (ϵ_2) for the even-even core $^{198}_{80}Hg$ is; $\epsilon_2 = 0.240$ and $\gamma = 32^0$. A value of $\Delta = 0.749MeV$ was obtained by the BCS calculation for the pairing gap. For the Fermi level, that calculation yielded, $\lambda_F = 52.6422MeV$.

iii. For $^{201}_{80}Hg$

A deformation parameter(ϵ_2) for the even-even core $^{201}_{80}Hg$ is; $\epsilon_2 = 0.110$ and $\gamma = 32^0$. A value of $\Delta = 0.661MeV$ was obtained by the BCS calculation for the pairing gap. For the Fermi level, that calculation yielded, $\lambda_F = 52.9268MeV$.

The results optained from the calculations have been tabulated as below.

a. Datas For $^{197}_{80}Hg$

Experimental data for$^{197}_{80}Hg$ [29];

$E_i(level)$	J_i^-	E_γ	I_i^-	E_f	J_f^-	Multi
557.77	$7^-/2$	250.2	<7	307.77	$5^-/2$	
”	”	405.8	<7	152.14	$3^-/2$	M_1
307.77	$5^-/2$	307.77	100	0.0	$1^-/2$	E_2
”	”	155.60	<2.73	152.14	$3^-/2$	
152.14	$3^-/2$	152.14	0	0.0	$1^-/2$	M_1

Table 4.1: Addopted Gamma levels for $^{197}_{80}Hg$.

The addopted gamma level data shown in Tab. (4.1) is the experimental data taken from litrature, and the Particle Tri-Axial Rotor Model calculation was made by treating the $^{197}_{80}Hg$ isotopes as a system of an even-even core plus an extra nucleon in a fixed deformation parameter.

Then, the obtained data was tabulated and labeled as shown in Fig. (4.1) and Fig. (4.2). The experimental data were tabulated and labeled side by side with the theoretical data, to compare the agreement between them.

Calculated Theoretical data for $^{197}_{80}Hg$;

J_i^-	E_i	E_f	J_f^-	ΔJ	E_γ	BE_2	BM_1	I_γ
$^{11}/_2^-$	1227.4	632.3	$^9/_2^-$	1	0.5951	0.0031	0.0191	100
		586.7	$^7/_2^-$	2	0.6407	0.5144	0	0.01818
$^9/_2^-$	632.3	586.7	$^7/_2^-$	1	0.0455	0	0.0253	100
		314.15	$^5/_2^-$	2	0.3175	0.0003	0	3.53325
$^7/_2^-$	586.7	314.15	$^5/_2^-$	1	0.2722	0.0128	0.0001	100
		147.6	$^3/_2^-$	2	0.4392	0.2822	0	0.00478
$^5/_2^-$	314.15	147.6	$^3/_2^-$	1	0.1669	0.0055	0.0593	100
		0.0	$^1/_2^-$	2	0.3145	0.3045	0	0.42303

Figure 4.1: Calculated data of $^{197}_{80}Hg$.

- The energy difference between the experimental and calculated values of each state is;

$$\triangle E_{\frac{9^-}{2}} = |E_{(\frac{9^-}{2})exp} - E_{(\frac{9^-}{2})theo}| = |632.3 - 715.36| = 83.06.$$

$$\triangle E_{\frac{7^-}{2}} = |E_{(\frac{7^-}{2})exp} - E_{(\frac{7^-}{2})theo}| = |557.77 - 586.7| = 28.93.$$

$$\triangle E_{\frac{5^-}{2}} = |E_{(\frac{5^-}{2})exp} - E_{(\frac{5^-}{2})theo}| = |314.15 - 307.77| = 6.38.$$

$$\triangle E_{\frac{3^-}{2}} = |E_{(\frac{3^-}{2})exp} - E_{(\frac{3^-}{2})theo}| = |147.6 - 152.14| = 4.54.$$

$$\triangle E_{\frac{1^-}{2}} = |E_{(\frac{1^-}{2})exp} - E_{(\frac{1^-}{2})theo}| = |0.0 - 0.0| = 0.0.$$

The energy difference calculation, between the experimental and the theoretical values, particularly in the low energy states were small compared to the higher energy states, and is in a good agreement with an error below 5% in average.

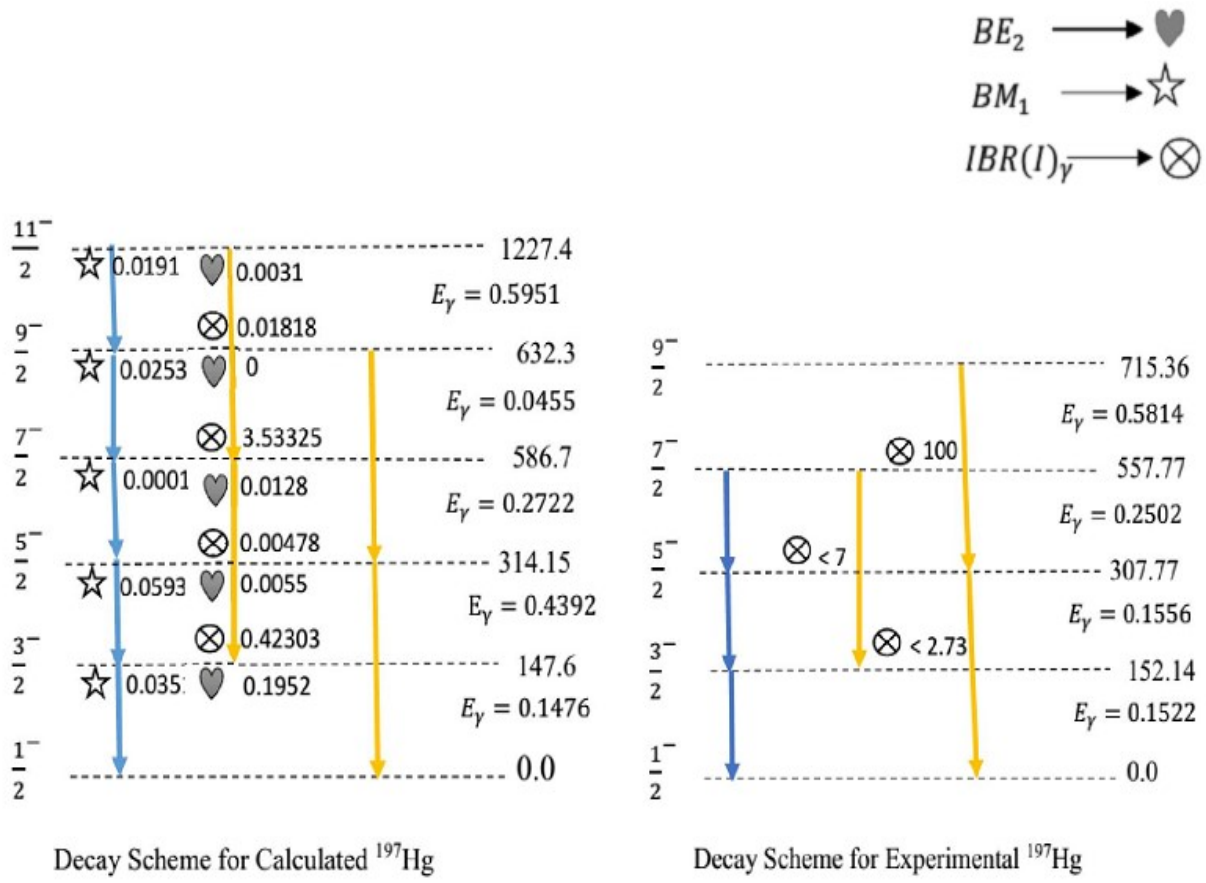

Figure 4.2: Decay level scheme for both Calculated and Experimental data of $^{197}_{80}Hg$.

- The gamma transition energy between different states are in a good agreement.

- When the variation of the branching ratio between the calculated and experimental values were compared; Even though, there were no complete experimental values of the branching ratio, the theoretical result shows a pronounced difference with it. As known, the exactness of the calculated value at large depends on the selection of the deformation parameter, there are also other sourses of errors to be mensioned. These are, may be either due to the selection of the even-even core, an error related to calculations (equations used) in the code may not acceptable for this nucleus or instrumental and personal errors.

b. Datas For $^{199}_{80}Hg$

Experimental data for$^{199}_{80}Hg$ [29];

$E_i(level)$	J_i^-	E_γ	I_i^-	E_f	J_f^-	Multi
667.6	$7^-/2$					
413.7	$5^-/2$	413.85	100	0.0	$1^-/2$	E_2
"	"	205.6	5	208.2	$3^-/2$	$[M_1, E_2]$
195.4	$3^-/2$	208.20481	100.0	0.0	$1^-/2$	$M_1 + E_2$

Table 4.2: Addopted Gamma levels for $^{199}_{80}Hg$.

Calculated theoretical data for $^{199}_{80}Hg$;

J_i^-	E_i	E_f	J_i^-	ΔJ	E_γ	BE_2	BM_1	I_γ
$^{11}/_2^-$	1016.2	684.1	$^9/_2^-$	1	0.3321	0.0034	0.0005	100
		666.6	$^7/_2^-$	2	0.3496	0.0003	0	25.542
$^9/_2^-$	684.1	666.6	$^7/_2^-$	1	0.0175	0.0379	0.0147	100
		423.7	$^5/_2^-$	2	0.2604	0.0001	0	0.94477
$^7/_2^-$	666.6	423.7	$^5/_2^-$	1	0.2429	0.1212	0.0091	100
		195.4	$^3/_2^-$	2	0.4712	0.1191	0	0.10469
$^5/_2^-$	423.7	195.4	$^3/_2^-$	1	0.2283	0.0227	0.0054	100
		0.0	$^1/_2^-$	2	0.4237	0.0111	0	0.70124
$^3/_2^-$	195.4	0.0	$^1/_2^-$	1	0.1954	0.0432	0.0063	100

Figure 4.3: Calculated data of $^{199}_{80}Hg$.

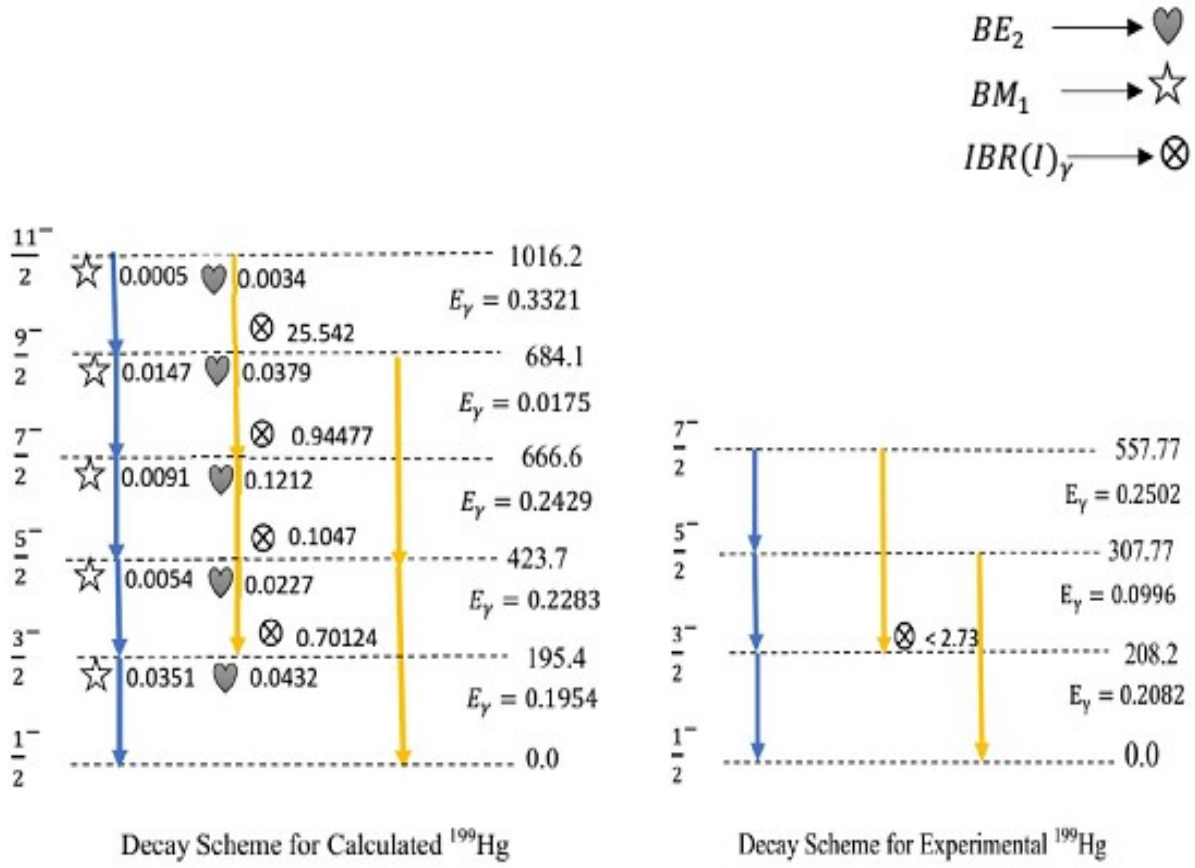

Figure 4.4: Decay level scheme for both Calculated and Experimental data of $^{199}_{80}Hg$.

The addopted gamma level data shown in Tab. (4.2) is the experimental data taken from litrature, and the PTRM calculations was made by treating the $^{199}_{80}Hg$ isotopes as a system of an even-even core plus an extra nucleon in a fixed deformation parameter.

Then, the obtained data was tabulated and labeled as shown in, Fig. (4.3) and Fig. (4.4) above. The experimental data were tabulated and labeled side by side with the theoretical data, to compare the agreement between them.

- The energy difference between the experimental and calculated values of each state was shown as;

$$\triangle E_{\frac{7^-}{2}} = |E_{(\frac{7^-}{2})exp} - E_{(\frac{7^-}{2})theo}| = |666.6 - 667.3| = 1.3.$$

$$\triangle E_{\frac{5^-}{2}} = |E_{(\frac{5^-}{2})exp} - E_{(\frac{5^-}{2})theo}| = |423.7 - 413.7| = 10.$$

$$\triangle E_{\frac{3^-}{2}} = |E_{(\frac{3^-}{2})exp} - E_{(\frac{3^-}{2})theo}| = |208.2 - 195.4| = 13.2.$$

$$\triangle E_{\frac{1^-}{2}} = |E_{(\frac{1^-}{2})exp} - E_{(\frac{1^-}{2})theo}| = |0.0 - 0.0| = 0.0.$$

As shown in the calculation the energy difference between the experimental and the theoretical values were made intensivelly, and they are in a good agreement with an error below 2% in average.

- The gamma transition energy between different states are in a good agreement.

- Even though, complete experimental datas were not found, the variation of the branching ratio between the calculated and experimental values were analysed and compared. Hence, it shows a pronounced difference. This difference was may be; due to the selection of the even-even core, an error related to calculations (equations used) in the code may not acceptable for this nucleus or instrumental and personal errors. The selection of the deformation parameters are also not forgotable.

c. Datas For $^{201}_{80}Hg$

Experimental data for$^{201}_{80}Hg$ [29]; The addopted gamma level data shown in Tab. (4.3)

$E_i(level)$	J_i^-	E_γ	I_i^-	E_f	J_f^-	Multi
414.539	$7^-/2$	382.45	82.8	32.145	$3^-/2$	E_2
384.6	$5^-/2$	352.42	100.0	32.145	$3^-/2$	$M_1(E_2)$
32.145	$3^-/2$	30.60	98.1	1.5648	$1^-/2$	$M_1 + E_2$

Table 4.3: Addopted Gamma levels for $^{201}_{80}Hg$.

is the experimental data taken from litrature, and the PTRM calculations was made by treating the $^{201}_{80}Hg$ isotopes as a system of an even-even core plus an extra nucleon in a fixed deformation parameter.

Calculated Theoretical data for $^{201}_{80}Hg$;

J_i^-	E_i		E_f	J_i^-	ΔJ	E_γ	BE_2	BM_1	I_γ
$^{11}/_2^-$	934.2	→	545	$^9/_2^-$	1	0.3892	0.0071	0.0066	100
		→	410.8	$^7/_2^-$	2	0.5233	0.0255	0	0.62135
$^9/_2^-$	545	→	410.8	$^7/_2^-$	1	0.1342	0.0992	0.0525	100
		→	383.6	$^5/_2^-$	2	0.1614	0.0160	0	106.37
$^7/_2^-$	410.8	→	383.6	$^5/_2^-$	1	0.0272	0.0447	0.0047	100
		→	44.8	$^3/_2^-$	2	0.366	0.0039	0	0.00533
$^5/_2^-$	383.6	→	44.8	$^3/_2^-$	1	0.3388	0.0126	0.0001	100
		→	1.3	$^1/_2^-$	2	0.3824	0.0036	0	2.1
$^3/_2^-$	44.8	→	1.3	$^1/_2^-$	1	0.0436	0.1801	0.0050	100

Figure 4.5: Calculated data of $^{201}_{80}Hg$.

Then, the obtained data was tabulated and labeled as shown in Tab. (4.3), Fig. (4.5) and Fig. (4.6) above. The experimental data were tabulated and labeled side by side with the theoretical data, to compare the agreement between them.

- The energy difference between the experimental and calculated values of each state was shown as;

$$\triangle E_{\frac{9^-}{2}} = |E_{(\frac{9^-}{2})exp} - E_{(\frac{9^-}{2})theo}| = |547.32 - 545| = 2.32.$$

$$\triangle E_{\frac{7^-}{2}} = |E_{(\frac{7^-}{2})exp} - E_{(\frac{7^-}{2})theo}| = |414.539 - 410.8| = 3.739.$$

$$\triangle E_{\frac{5^-}{2}} = |E_{(\frac{5^-}{2})exp} - E_{(\frac{5^-}{2})theo}| = |384.6 - 383.6| = 1.$$

$$\triangle E_{\frac{3^-}{2}} = |E_{(\frac{3^-}{2})exp} - E_{(\frac{3^-}{2})theo}| = |32.145 - 44.8| = 12.655.$$

$$\triangle E_{\frac{1^-}{2}} = |E_{(\frac{1^-}{2})exp} - E_{(\frac{1^-}{2})theo}| = |1.5648 - 1.3| = 0.2648.$$

In this case, the theoretical calculation has very small difference with the experimental

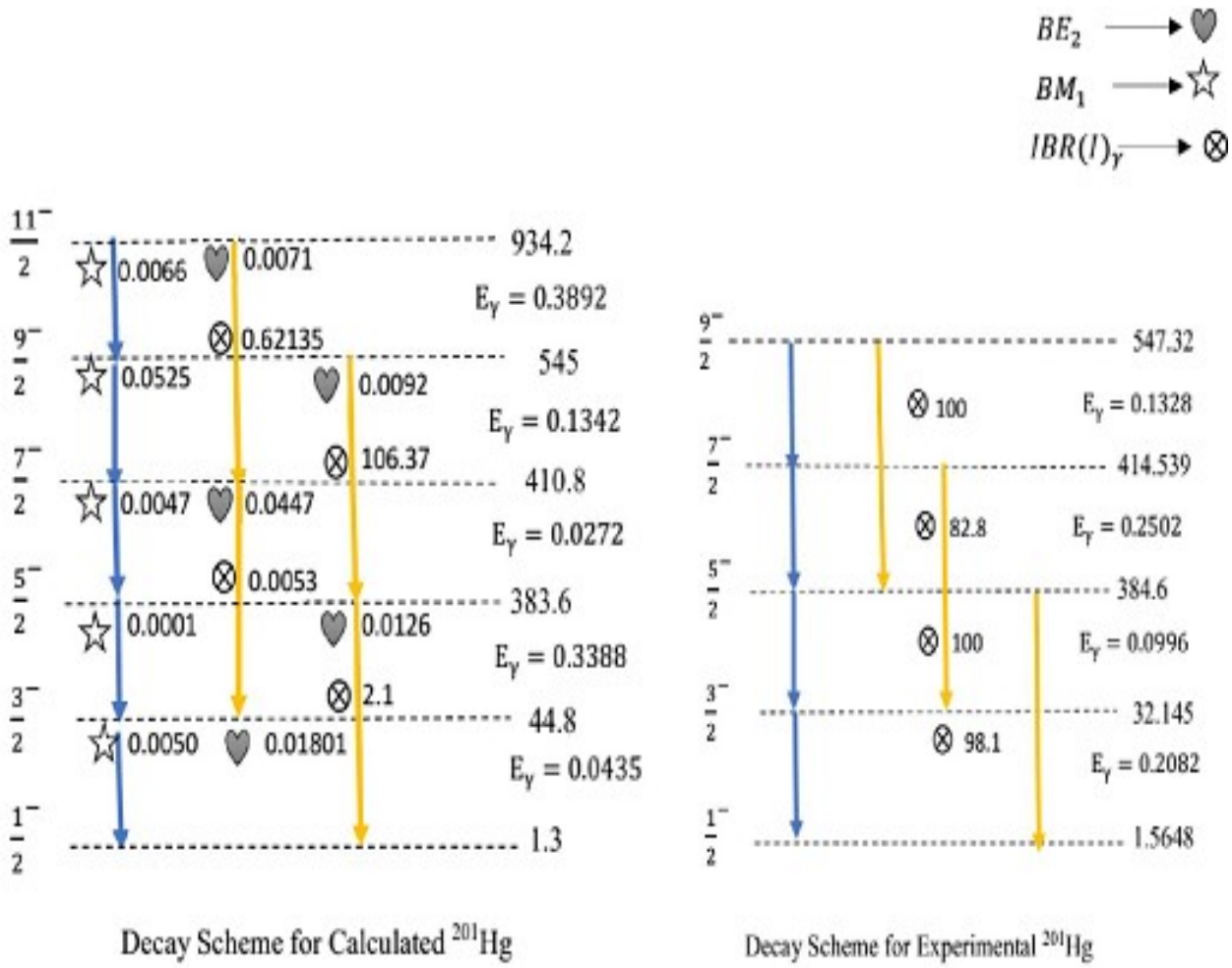

Figure 4.6: Decay level scheme for both Calculated and Experimental data of $^{201}_{80}Hg$.

values. Hence, the experimental and the calculated theoretical level energies were in a good agreement with an error below 10% in average.

- The gamma transition energy between different states are in a good agreement.
- When the variation of the branching ratio between the calculated and experimental values were compared; Even though, there were no complete experimental values, it shows a pronounced difference. This difference was may be; due to the selection of the even-even core, in effective determinantion of the deformation parameters, an error related to calculations (equations used) in the code may not acceptable for this nucleus or instrumental and personal errors.

5

Conclusion

In this thesis, the Low lying state for negative parity odd-A isotopes of Hg were studied, by using the Particle Plus Tri-Axial Rotor Model with the associated computer codes (GAMPEN, ASYRMO, PROBAMO). In this method, the quantum many body system of a nucleus were changed in to two body system (by considering a single nucleon and an even-even core), it also used to neglect some of the parameters by approximation and was effective in low energy states. The Level Energies, Gamma Transition Energy, Transition Intensity (Branching ratio), Electromagnetic Transitions(EM_1 and EM_2) and Magnetic Transitions (BM_1) was calculated for each particular deformation parameters(ϵ_2) and γ of the respective isotopes. The results of the calculations are also summarized and compared with experimental results as shown in Fig. (4.1) to Fig. (4.6), respectively.

Over all in this work, in all aspects of the theoretical calculations a reasonable result with an error less than 8% in average was obtained. These discrepancies between theory and experiment might be due to the choice of the deformation parameters, selection of the even-even core, an error related to calculations (equations used) in the code (may not acceptable for this nucleus) or instrumental and personal errors.

In addition the result aserts that, the model is a good theoretical approach to produce the main feature of the experimental level scheme and so does to calculate the low

lying negative parity odd-A isotopes of Mercury structure parameters, intern to study it's nuclear structure, suggesting that a more intensive study of this method is required for a more accurate of its understanding and description.

Reference

[1] S. A. Moszkowski, (1957), *Structure of Atomic Nuclei*, Springer-Verlag, Berlin Heidelberg,

[2] S. A. Moszkowski, (1957), Models of Nuclear Structure, Springer, Berlin Heidelberg, 8/39.

[3] Hulthen,L. and M. Sugawara, (1957), The Two body nucleon problem, 39.

[4] Proceedings of the DAE-BRNS Symp. on Nucl. Phys, (2015), Study of low-spin states of $^{(197)}Hg$ from decay spectroscopy, 60.

[5] University of GUELPH,Physics Department, (2015), Nuclear Structure, Nuclear physics group.

[6] M. G. Mayer, Phys. Rev. 75, 1969 (1949). 0. Haxel, J. H. D. Jensen, and H. E. Suess, Phys. Rev. 75, 1766 (1949). M. G. Mayer and J. H. D. Jensen, *Elementary Theory of Nuclear Shell Structure*, John Wiley and Sons, Inc., New York.

[7] R. F. Casten, (1990), *Nuclear Structure from a Simple Perspective*, Oxford University Press, New York.

[8] Daniel Koller, (2012), Introduction to Nuclear Models, Massachusetts Institute of Technology.

[9] S. 0. Milsson, Mat. Fys. Medd. Ban. Vid. Selsk. (1970), The deformed spin-orbit potential in Nilsson-model calculations, 142(1).

[10] Kenneth S. Krane, John Wiley Sons, Inc. (1988),*Introductory Nuclear Physics*, Oregon State University.

[11] Prof. Robert J. Lancashire, (2003), Nuclear energy level, The Department of

Chemistry, India.

[12] Peter Ring, Peter Schuck, (1980), *The Nuclear Many-Body Problem*, New York Heidelberg Berlin.

[13] A. Bohr and B. R. Mottelson, (1998), Nuclear Structure, 1.

[14] P. Petkov, P. von Brentano, J. Jolie, and R. V. Jolos, Particle-Triaxial Rotor Calculations around 195-Pt, 1090.

[15] https://www.britannica.com/science/radioactivity/Nuclear models/Encyclopedia Britannica.

[16] Girija. K.K., (2012), *Studies of shape changes of deformed nuclei and its effects on cluster emission*, Department of Physics, University of Calicut.

[17] Samuel S. M. Wong, (2007), *Introductory Nuclear Physics*, Prentice - Hall of India, Pvt. Ltd, New Delhi.

[18] Ashok K. Jain and P. Arumugam, (2006), *Mean field description of nuclei*, Narosa Publishing House, New Delhi.

[19] K. Heyde, (1998), *Basic ideas and concepts in Nuclear physics - An introductory approached*, (Overseas Press, India, Pvt. Ltd.).

[20] Frank S. Stephens Nuclear Science Division, Lawrence Berkeley Laboratory, University Of California, Berkeley, Ca 94720, U.S.A. Part 1, *Collective Bands In Some Rotational And transitional Nuclei.*

[21] (2018), Nuclear Science- A Guide to the Nuclear Science Wall Chart, Fourth Edition.

[22] I. Rangrarson, (1992), *THE PARTICLE + TRIAXIAL ROTOR MODEL: A USER'S GUIDE*, Sweden.

[23] R.R. Roy and B.P. Nigam, (1996), *Nuclear Physics - Theory and Experiment*, (New Age International (P) Ltd).

[24] W. Nazarewicz and I. Ragnarsson, (2008), *A Handbook of Nuclear Properties*, Dorin

N.Poenaru, Walter Greiner, (Oxford University Press, New York) p. 80.

[25] Ashok K. Jain and P. Arumugam, (2006), *Mean field description of nuclei*, Y.K. Gambhir (Narosa Publishing House, New Delhi) p.115.

[26] John Lilley,(2002), *Nuclear Physics - Principles and applications*, D.J. Sandiford, F. Mandl, A.C. Phillips (John Wiley Sons, Ltd, New York).

[27] O. Haxel, J.H.D. Jensen and H.E. Suess, Phys. Rev. 75, (1949) 1766.

[28] Gerda Neyens,(2006), REPORTS ON PROGRESS IN PHYSICS, INSTITUTE OF PHYSICS PUBLISHING, Nuclear magnetic and quadrupole moments for nuclear structure research on exotic nuclei.

[29] Brookhaven National Laboratory Data center, 2019, Evaluated Nuclear Structure Data File Searchand Retrival(ENSDF).

[30] Naoki Tajima and Norifumi Suzuki,(2001), Phys. Rev. C64, 037301.

[31] Raymond A. Sorensen, (1973) Rev. of Modern Physics 45(3).

[32] Sven Gosta Nilsson and Ingemar Ragnarsson, (1995), Shapes and shells innuclear struc-ture, (Cambridge University Press, Cambridge).

[33] B. R. Martin (2006). Nuclear and Particle Physics. John Wiley Sons, Ltd.

[34] P. Petkov 1,2,a , P. von Brentano 1 , J. Jolie 1 , and R.V. Jolos 3, (2008), Particle-triaxial rotor calculations for the low-lying states with negative parity in $^{(193)}Os$ (Springer-Verlag).

[35] B. Castel and I.S. Towner, (1990), Modern Theories of Nuclear Moments (Clarendon Press, Oxford).

[36] K.L.G. Heyde, (1994), The Nuclear Shell Model, 2nd ed. (Springer, Berlin Heidelberg).